ELSEVIER

Journal of Organometallic Chemistry 556 (1998) 229–238

Journal of Organometallic Chemistry

Bis(cyclopentadienyl)lanthanoid(III) alkoxides derived from chiral alcohols with a nitrogen donor functionality: Solution NMR studies of paramagnetic complexes

Annette Steudel [a], Eric Siebel [a], R. Dieter Fischer [a,*], Gino Paolucci [b], Vittorio Lucchini [c]

[a] *Institut für Anorganische und Angewandte Chemie, Universität Hamburg, Martin-Luther-King-Platz 6, D-20146 Hamburg, Germany*
[b] *Dipartimento di Chimica, Università di Venezia, Dorsoduro 2137, I-30123 Venezia, Italy*
[c] *Dipartimento di Scienze Ambientali, Università di Venezia, Dorsoduro 2137, I-30123 Venezia, Italy*

Received 19 November 1997

Abstract

The first crystallographically elucidated example of a chiral organolanthanoid alkoxide complex $[LnCp'_2(\mu\text{-}OCHRCHR^1NR^2R^3)]_2$ with Ln = Sm, R = Ph, R^1 = H, R^2 = Me and $R^3 = CH_2Ph$ (**11**; prepared from the pure (1R)-(+)-aminoalcohol) is presented. While crystalline **11** involves distinct N–Sm bonds (283.3 pm) in enantiomorphic {(-CHPhCH_2)(CH_2Ph)MeN–Sm} fragments, its solution NMR spectra (^{1}H, ^{13}C) suggest a complete or partial rupture of the N–Sm bonds. More systematic solution ^{1}H-NMR studies of likewise chiral representatives of the series with R = H, R^1 = Et, R^2, R^3 = Me and Ln = Pr, Nd, Sm, Yb and Lu, respectively, indicate that at room temperature (r.t.) only the dissolved complexes with Ln = Pr, Nd and Sm involve N–Ln bonds that are stable on the NMR time scale. The homologues with Ln = Yb and Lu are fluxional. The paramagnetic nature of the complexes with Ln = Pr, Nd and Yb turns out to be particularly helpful for the structural deductions in magnifying significantly e.g. the diastereotopic splitting of the ring proton resonances of various $CH_3C_5H_4$ ligands.

Keywords: Alkoxide complex; NMR spectra; Chiral ligand

1. Introduction

In close analogy to several dialkylaluminium alkoxides $[R_2AlOR']_2$ [1], the cyclic $\{Ln_2O_2\}$ core of dinuclear bis(cyclopentadienyl)lanthanoid(III) derivatives involving a donor-functionalized alkoxide ligand μ-(O-**X**-D) (D = Lewis basic donor group) may expand to a tricyclic skeleton. While the more rigid form **B** (Fig. 1) is usually realized in the crystalline state [2], various isomers may coexist in solution. The present contribution is focused mainly on the still less explored solution behaviour of representatives of the new sub-class $[Cp'_2LnOCHRCHR'(NMe_2)]_2$ with $Cp' = \eta^5\text{-}C_5H_5$ or $\eta^5\text{-}C_5H_4Me$, R = H, R′ = Et or H and Ln = Pr, Nd, Sm, Yb, and Lu. As the first crystallographically elucidated example containing a nitrogen donor, we also include the (slightly modified) complex $[Sm(C_5H_5)_2(\mu\text{-}OCH(Ph)CH_2NMeCH_2Ph]_2$ along with its Pr- and Yb-homologues. Moreover, the comparison with two complexes carrying a methyl group instead of the NMe_2 donor functionality was expected to be quite informative for the present study. All compounds considered in this investigation were prepared for the first time and are listed in Table 1.

The presence of a chirogenic centre in the alkoxide ligands DMAB, BMPE and MB was important both for successful NMR spectroscopic analyses and in view of potential chiroptic responses by the 4f electrons of complexes with a partially filled 4f sub-shell [3] to be presented in a subsequent paper. With the exception of

* Corresponding author. Fax: +49 404 1232893.

0022-328X/98/$19.00
PII S0022-328X(98)00378-7

compound **6**, all new complexes contain a paramagnetic lanthanoid(III) ion. Hence, most of the NMR spectra considered should in principle be affected by the long-known advantages and limitations, respectively, caused by the presence of unpaired 4f-electrons [4].

2. Results and discussion

2.1. Synthesis and general product characterization

All alkoxide systems were prepared by well-controlled low-temperature protolysis of the corresponding $LnCp'_3$ complexes with H-DMAB, H-DMAE, H-BMPE and H-MB, respectively:

$$LnCp'_3 + DCHR'CHROH$$

$$\rightarrow \tfrac{1}{2}[Cp'_2LnOCHRCHR'D]_2 + Cp'H$$

All products were obtained analytically pure and are satisfactorily soluble (e.g. for the NMR studies) in CH_2Cl_2. Nevertheless, the very complex room temperature (r.t.) ^{1}H-NMR spectra of **10**–**12** could so far not satisfactorily be interpreted although the somewhat simpler ^{13}C-NMR spectrum of **11** (Table 7) clearly

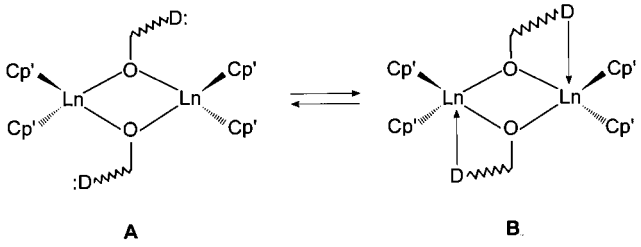

Fig. 1. Structural alternatives of $[Cp'_2Ln(\mu\text{-}O\text{–}D)]_2$ systems (schematic view; D = Lewis basic donor group).

Table 1
List of all $[Cp'_2Ln(alkoxide)]_2$ complexes considered (**7** = pure alcohol)

Number	Ln	Cp′-ligand	Alkoxide ligand	Colour
1	Pr	C_5H_5	DMAB[a]	Light green
2	Pr	$CH_3C_5H_4$	DMAE[b]	Light green
3	Nd	$CH_3C_5H_4$	DMAB	Light blue
4	Sm	C_5H_5	DMAB	Bright yellow
5	Yb	C_5H_5	DMAB	Orange
6	Lu	C_5H_5	DMAB	Pale brown
7	–	–	H-DMAB	Colourless
8	Pr	$CH_3C_5H_4$	MB[c]	Pale green
9	Yb	$CH_3C_5H_4$	MB	Orange
10	Pr	C_5H_5	BMPE[d]	Pale green
11	Sm	C_5H_5	BMPE	Yellow
12	Yb	C_5H_5	BMPE	Orange

[a] H-DMAB = (R)-(-)-2-(*N*-dimethylamino)butanol.
[b] H-DMAE = 2-(*N*-dimethylamino)ethanol.
[c] H-MB = (S)-(-)-2-methylbutanol.
[d] H-BMPE = (R)-(+)-2-(*N*-methylbenzylamino)-1-phenylethanol.

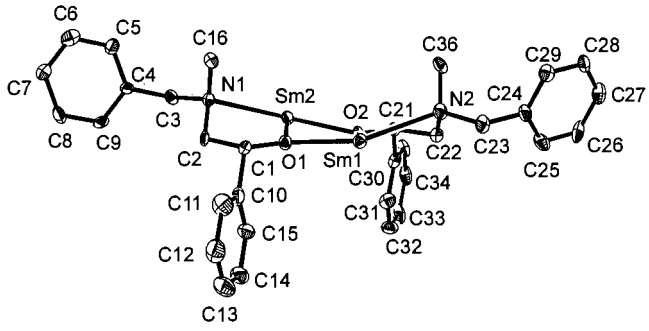

Fig. 2. ORTEP plot (30%) of the molecular structure of **11** and complete atomic numbering scheme. The four C_5H_5 ligands have been omitted for clarity.

Table 2
Selected bond distances (pm) and angles (°) of **11** (cent = C_5H_5 ring centre)

Sm1–cent1	251.3(3)	Sm2–cent3	251.4(3)
Sm1–cent2	252.8(3)	Sm2–cent4	251.7(3)
Sm1–N2	283.4(12)	Sm2–N1	283.7(11)
Sm1–O1	246.3(9)	Sm2–O2	247.8(9)
Sm1–O2	232.8(9)	Sm2–O1	235.3(9)
Sm1···Sm2	393.5(5)		
O1–Sm1–O2	68.8(3)	O1–Sm2–O2	68.2(3)
O2–Sm1–N2	67.1(3)	O1–Sm2–N1	66.8(3)
O1–Sm1–N2	133.6(3)	O2–Sm2–N1	132.1(3)

shows only one Cp carbon resonance. Correspondingly, **11** displays at r.t. only one reasonably intense resonance assignable to the Cp protons, but probably two signals at −70°C (vide infra). On the other hand, most of the proton resonances of **1**–**9** could unambiguously be assigned (see Tables 4 and 5). Attempts to arrive at single crystals suitable for crystallographic X-ray studies have so far been successful only in the case of complex **11**.

2.2. Crystal structure of $[Sm(C_5H_5)_2(\mu\text{-BMPE})]_2$, *11*

The low-temperature single-crystal X-ray analysis of **11** confirms the expected dinuclear nature and documents that, at least in the solid state, distinct metal-to-nitrogen bonds exist (Fig. 2). Most probably owing to steric congestion, the Sm–N distance of 283.3 pm is comparatively long, and it appears uncertain if a permanent Sm–N bond will survive when the complex is dissolved in a polar solvent like CH_2Cl_2. Sm–N bonds of similar lengths (281.6 and 284.4 pm) have, nevertheless, been reported for a complex containing a pyridyl-functionalized samarium alkoxide complex [5,9], although values closer to that found e.g. for $[Sm(C_5H_5)_3(C_5H_5N)]$ (265.6 pm [6]) must be considered as more common. Selected bond distances and angles of **11** are given in Table 2, and important crystal parameters in Table 3. Interestingly, the Sm–O dis-

tances of **11** are likewise notably longer than in other samarium alkoxide complexes [5]. The two α-phenyl groups are oriented *cisoid* and approximately perpendicular to the tricyclic skeleton. The same is true for the *N*-bonded methyl groups, with the result that even both nitrogen atoms of solid **11** have become chirogenic centres of only one well-defined configuration. Thus, only one distinct diastereomeric form of **11** is realized in the crystal. Obviously, the two Cp′ ligands of each Sm(III) ion (not shown in Fig. 2) are nonequivalent. While the tricyclic skeleton of **11** is nonplanar (Fig. 2), the three ligator atoms in the equatorial girdle of each mononuclear complex fragment lie approximately in one plane.

2.3. Room temperature NMR studies of *1–9*

A comparison of the NMR data of the two donor-free type **A** systems **8** and **9** with those of their potential type **B** counterparts **1** or **2** (Ln = Pr) and **5** (Ln = Yb), respectively, reveals throughout surprising differences in the actual positions of the resonances of chemically equivalent protons (see Tables 4 and 5). For better clarity, also the average values of all resonances belonging to related protons of the potential **B**/**A** pairs **1**/**8** and **5**/**9** are compared in Table 6. Interestingly, the isotropic shifts (of either sign) of all protons of the NMe_2-free systems turn out to be strongly increased when compared with those of the potential type **B** systems, which feature suggests significant changes in the anisotropy of the magnetic susceptibility of both the Pr^{3+} and the Yb^{3+} ion, when one of the three coordination sites in the equatorial girdle of a type **B** system becomes vacant. As even protons separated from the paramagnetic centre by more than three σ-bonds are notably affected, delocalization of free spin density (causing different Fermi contact shifts) is probably not the dominant factor.

Table 3
Summary of crystal data and details of data collection and refinement for **11**

Empirical formula (with solvent)	$C_{69.5}H_{76}N_2O_2Sm_2$
Formula weight	1272.02
Temperature (K)	153(2)
Diffractometer	Hilger and Watts Y290
Wave length (pm)	71.073
Crystal system	Monoclinic
Space group	$P2_12_12_1$
Unit cell dimensions (pm)	
a	1404.9(5)
b	1917.0(6)
c	2570.0(3)
Volume ($\times 10^6$ pm^3)	6921.0(8)
Z	4
Density (calc.) (g cm^{-3})	1.221
Absorption coefficient (cm^{-1})	1.720
F(000)	2588
θ-range for data collection (°)	2.27–27.55
Reflections collected	6605 [$I>2\sigma(I)$]
Independent reflections	6170 [R(int) = 0.0170]
Data/restraints/parameters	6168/9/551
Final *R*-indices	$R_1 = 0.0493$, $wR_2 = 0.1417$
R-indices (all data)	$R_1 = 0.0603$, $wR_2 = 0.1522$
Absolute structure parameter	−0.03(3)
Largest difference peak and hole (nm^{-3})	1.189 and −0.491 e $\times 10^{-6}$ pm^3

More straightforward criteria to distinguish between a rigid type **B** dimer and its more fluxional type **A** isomer by NMR spectroscopy make use of the dissymmetry of the β-carbon atom in the DMAB and MB ligands. In the presence of one distinct DMAB-enantiomer, just one type **B** configuration [7] with two nonequivalent *N*-bonded methyl groups and Ln-bonded Cp′-ligands, respectively, is expected, since the two β-positioned ethyl groups should adopt a *cisoid* orientation (like the α-phenyl groups in the structure of **11**). In contrast, in the absence of a N–Ln bond (type **A**), neither of the two fragments $\{Cp'_2Ln(O)_2\}$ and $\{Me_2NCH_2\}$ will even be prochiral, so that diastereotopic splitting of the Cp′-and Me-resonances cannot take place in spite of two close-lying chirogenic centres [8]. The protons of the α- and γ-CH_2 groups, respectively, of the DMAB and MB ligand are likewise nonequivalent in isomer **B**, but remain prochiral in isomer **A**, so that diastereotopic splitting of their CH_2 resonances can be no stringent argument for the presence of form **B**.

The appearance of two resonances of the *N*-bonded methyl groups in the spectra of the complexes **1**, **3** and **4**, but of only one singlet in the spectra of **5**, **6** and **7** (Table 5) immediately suggests that *N*-coordination seems to be favoured in the case of the lighter Ln^{3+} ions, most probably owing to their comparatively larger ionic radii. This view is supported by the appearance of two C_5H_5 proton resonances in the spectra of **1** (see also Fig. 3) and **4**, but of only one signal in the spectra of **5** and **6** (Table 4). Complex **2** which is expected to adopt type **B**, too, lacks a dissymmetric C-atom so that the above criteria cannot be applied. Yet, as here the C_5H_5 ligand is replaced by its $CH_3C_5H_4$ derivative, another way of arguing becomes applicable. The somewhat idealized Newman projection (Fig. 4) viewed along one of the cent → Pr vectors (cent = centre of the $CH_3C_5H_4$ ring in question) demonstrates that each (rapidly rotating, vide infra) $CH_3C_5H_4$ ligand involves two prochiral pairs of ring protons (in the positions 1/1′ and 2/2′, respectively) whose resonances should experience significant diastereotopic splitting in the presence of the N–Pr bond. Experimentally, **2** displays only one low-field CH_3 resonance confirming equivalence of the two $CH_3C_5H_4$ ligands, and four widely spaced C_5H_4 ring proton resonances in accordance with pronounced diastereotopic splitting. In contrast, isomer **B** of complex **3** should involve two non-equivalent $CH_3C_5H_4$

Table 4
Room temperature ^{1}H-NMR data (chemical shifts in ppm) of the C_5H_5 and $CH_3C_5H_4$ protons of the complexes **1**–**6** and **8**, **9**

Sample	Ln	CH_3-resonances	C_5H_5/C_5H_4-resonances[a]			
1	Pr	–	12.55 (5H)		0.71 (5H)	
2	Pr	9.75 (6H)	15.85 (2H)	11.06 (2H)	4.66 (2H)	−4.20 (2H)
3	Nd	11.79 (3H), 9.75 (3H)	11.8 (1H)	4.06 (1H)	2.08 (1H)	−8.15 (1H)
			7.22 (1H)	0.41 (1H)	−3.35 (1H)	−14.40 (1H)
4	Sm	–	8.79 (5H)		8.59 (5H)	
5	Yb	–	−24.01 (10H)			
6	Lu	–	5.99 (10H)			
8	Pr	−0.85 (6H)	25.87 (2H)	25.72 (2H)	25.31 (2H)	24.19 (2H)
9	Yb	27.60 (6H)	−81.73 (2H)	−80.05 (2H)	−78.74 (2H)	−77.06 (2H)

[a] The order of the ring proton shifts is plausible, but still tentative.

ligands and, in excellent agreement with our expectation, now the appearance of two ring methyl resonances and eight widely spaced, equally intense C_5H_4 proton lines (Table 4) signalizes the presence of N–Pr bonds.

Strictly speaking, the resonances of the $CH_3C_5H_4$ ring protons should experience diastereotopic splitting even in the absence of the N–Ln bond, as long as the alkoxide ligand contains a dissymmetric carbon atom. Thus, the two type **A** complexes **8** and **9** display, like **2,** one CH_3 and four C_5H_4 resonances each (Table 4). However, owing to the absence of the N–Ln bond, the two cyclic ligands remain equivalent (i.e. only one methyl resonance is observed), and the much longer separation of the chiral β-carbon atom from the prochiral proton pairs in **8** and **9** causes a drastic reduction of the diastereotopic splitting (see Table 4). On the other hand, the magnitude of the splitting of the α- and γ-CH_2 resonances of the (type **A**) systems **8** and **9** even exceeds that displayed by the type **B** systems **1** and **5** (Table 5), confirming that this particular feature of the NMR spectrum cannot be used to unambiguously identify type **B** systems.

While the ^{1}H-NMR spectrum of the paramagnetic Sm(III) system **4** leaves again no doubt in a predomi-

Table 5
Room temperature ^{1}H-NMR data of the alkoxide ligand (chemical shifts in ppm) of the compounds **1**–**9**

Sample	Ln	NMe_2/2-Me	α-CH_2	β-$CH_{1/2}$	γ-CH_2	δ-CH_3
1	Pr	−30.58 (3H)	−13.47 (1H)	−0.32 (1H)	−12.7m (1H)	−4.64t (3H)[b]
		−33.95 (3H)	−6.66 (1H)[a]		−10.0m (1H)	
2	Pr	−27.98 (6H)	−18.81 (2H)	−15.01 (2H)	–	–
3	Nd	−15.99 (3H)	−9.67 (1H)	−9.29 (1H)	−4.99 (1H)	−4.35 (3H)
		−15.83 (3H)	−9.10 (1H)		−5.22 (1H)	
4	Sm	0.18 (3H)	−1.52m (1H)	Not detected	−0.50m (1H)	−0.27t (3H)
		−1.27 (3H)	−2.03t (1H)[c]		−1.00m (1H)	
5	Yb	69.60 (6H)[d]	77.94 (1H)	ca. 71	39.61 (1H)	18.66 (3H)
			67.42 (1H)		33.37 (1H)	
6	Lu	2.42 (6H)	3.90dd (1H)[e]	2.34m (1H)	1.68m (2H)	1.06d (3H)[f]
			3.52t (1H)[g]			
7		2.27 (6H)	3.56dd (1H)[h]	2.50sept (1H)[k]	1.60m (1H)	0.89t (3H)
			3.22t (1H)[m]		1.10m (1H)	
8	Pr	−43.60 (3H)	−90.3 (1H)	−40.91 (1H)	−58.64 (1H)	−21.08 (3H)
			−97.7 (1H)		−69.51 (1H)	
9	Yb	92.13 (3H)	256.3 (1H)	251.5 (1H)	110.23 (1H)	53.22 (3H)
			285.9 (1H)		93.07 (1H)	

[a] $\Delta H_{1/2}$, 23.3 Hz.
[b] $^3J = 7$ Hz.
[c] $^3J = 10$ Hz.
[d] Two faintly emerging maxima.
[e] *Cisoid* to Et; $^2J = 7.3$ Hz, $^3J = 4.7$ Hz.
[f] *Transoid* to Et; $^{2,3}J = 11.3$ Hz.
[g] 360 MHz, $CDCl_3$.
[h] $^2J = 10.5$ Hz, $^3J = 4.9$ Hz.
[k] $^3J = 4.6$ Hz.
[l] $^3J = 7.5$ Hz.
[m] *Transoid*, $^{2,3}J = 10.3$ Hz.

Table 6
Comparison of the averaged ^{1}H-NMR shifts (in ppm) of chemically corresponding protons in potential type **B** (**1**, **5**) and type **A** (**8**, **9**) systems, respectively

Sample	Ln	CH_3	$C_5H_{4/5}$	α-CH_2	β-$CH_{1/2}$	γ-CH_2	δ-CH_3
1	Pr	–	6.63	−10.06 (6.81)	−0.32	−11.39 (2.64)	−4.64
8	Pr	−0.85	25.27	−94.0 (7.4)	−40.91	−64.07 (10.87)	−21.08
5	Yb	–	−24.01	72.68 (10.52)	ca. 71	36.49 (6.24)	18.66
9	Yb	27.6	−79.39	271.12 (29.6)	251.5	101.65 (17.16)	53.22

In parentheses: magnitude of corresponding diastereotopic splitting (in ppm).

nance of isomer **B** over **A** (vide supra), the actual isotropic NMR shifts are, as usually in the case of Sm(III) complexes [9], quite weak. Moreover, the r.t. ^{13}C-NMR shifts of **4** (and **11**, see Table 7) are surprisingly similar to those of the diamagnetic homologue **6** (Ln = Lu), although the C_5H_5 carbon atoms of **4** and **11** immediately contact the paramagnetic metal ion. Surprisingly, the two *N*-bonded methyl carbon atoms of **4** give rise to only one ^{13}C singlet in spite of the appearance of two methyl proton resonances (Table 5), while both the r.t. ^{13}C and ^{1}H resonances of the C_5H_5 ligands of the sterically more congested complex **11** (vide supra) are indicative of type **A**.

Likewise, the r.t. ^{1}H-NMR spectra of both **5** and **6** (Ln = Yb and Lu) as well as the ^{13}C-NMR spectrum of **6** clearly signalize the presence of the fluxional form **A**. The appearance of one rather broad NMe_2 proton resonance (see Fig. 8a) suggests that the fluxionality of **5** may be restricted to temperatures above 20°C. Interestingly, the α-CH_2 protons of both **6** and **7** give rise to one double doublet and one triplet (Table 5 and Fig. 5). Assuming here for the $\{C^{\alpha}H_2C^{\beta}H(Et)\}$ fragment in the chelating ring of **6** a synperiplanar conformation as depicted by the Newman projection shown in Fig. 6, a quasi-triplet could be attributed to the α-CH_2 proton *transoid* to the ethyl group, provided that geminal and vicinal coupling with almost equal, and relatively large

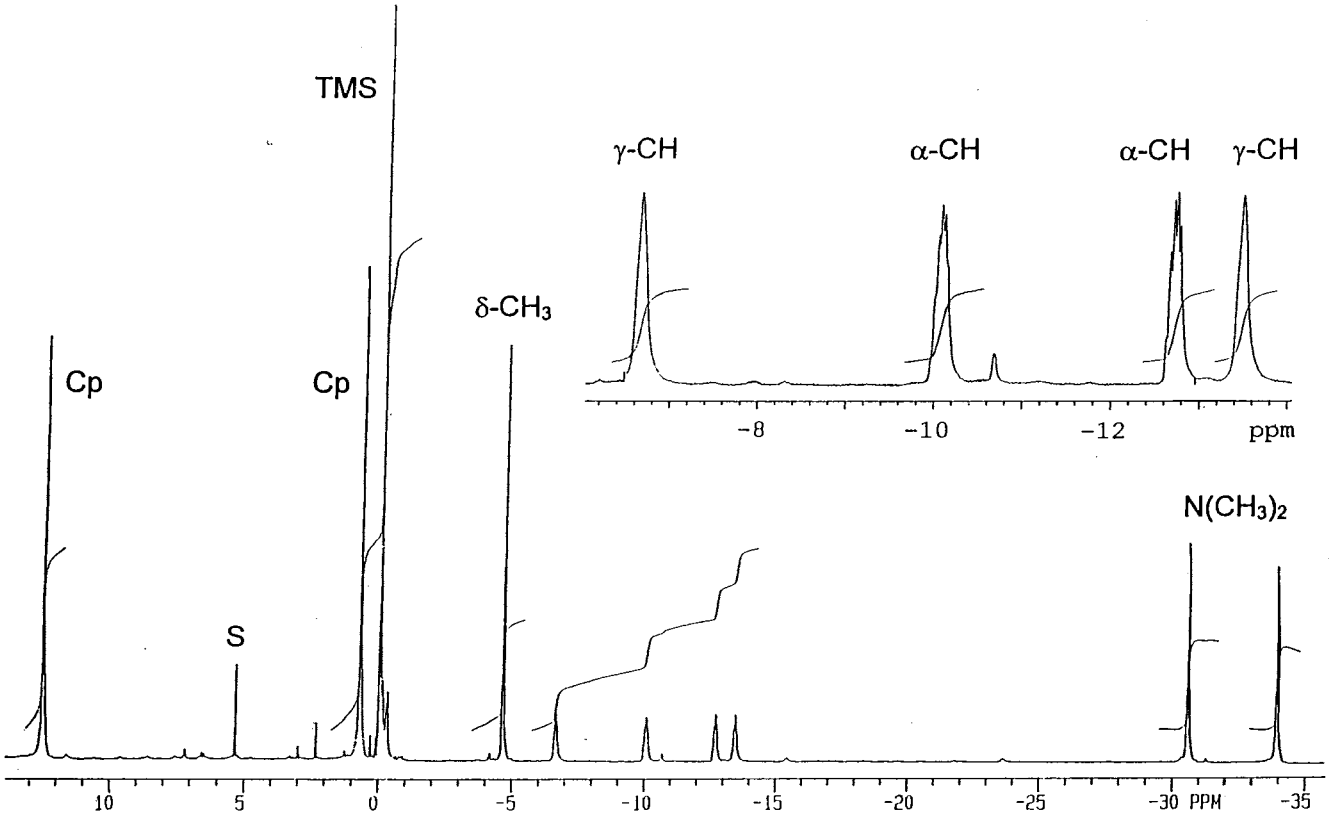

Fig. 3. Room temperature ^{1}H-NMR spectrum of **1** (Ln = Pr).

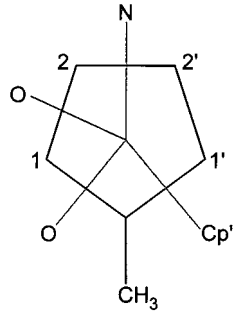

Fig. 4. Newman projection of one $\{(CH_3C_5H_4)^{1,2}_2Ln(O)^1(O)^2N\}$ fragment of isomer **B** of **2** or **3**, viewed along its cent$^1 \rightarrow$Ln vector (cent = $CH_3C_5H_4$ ring centre).

coupling constants (of ca. 11.3 Hz) may be anticipated. The double doublet should then result from both geminal and vicinal coupling of the *cisoid* CH_2 proton with two notably different coupling constants (of about 11.9 and 4.7 Hz, respectively). A non-planar five-membered ring in which the $C^{\alpha} \rightarrow H$ (*transoid*) and $C^{\beta} \rightarrow H$ vectors span a dihedral angle of almost 0° was actually found crystallographically for the quasi-homologue of **5** with $Cp' = CH_3C_5H_4$ and $D = OCH_3$ instead of $N(CH_3)_2$ ([10]a). On the basis of Karplus' equation [11], corresponding estimates of J(H,H) did in fact result ([10]b). Consequently, in spite of the appearance of only one C_5H_5 and $N(CH_3)$ resonance, the specific multiplet pattern of the α-CH_2 protons of **6** discloses the existence of (at room temperature only short-lived) N–Lu bonds. In contrast, the intramolecular N–Lu bonds of the recently described [12], likewise chiral complexes $[Me_2Si(C_5Me_4)(C_5H_3CH_2CH_2NMe_2)LuR]$ (R = Cl, Me) were found to be stable even in solution. Anticipating an intramolecular hydrogen bond, the pure alcohol **7** could involve a relatively labile, five-membered ring, too (see Fig. 7).

2.4. Low-temperature NMR results for **5**, **6** and **11** and outlook

While (ignoring here its *N*-methyl ^{13}C singlet) the Sm-complex **4** behaves as a type **B** system, its sterically slightly more congested derivative **11** seems to prefer the fluxional form **A** (vide supra). At −80°C, however, the number of medium intense, sharp resonances in the ^{1}H-NMR spectrum of **11** has strongly increased. Yet, all that might be deduced from the already complicated r.t. spectrum is that probably more than one C_5H_5 proton resonances appear between 2.5 and 7.5 ppm, so that here the presence of at least two comparatively long-lived species cannot be ruled out.

In contrast to **11**, the two DMAB-containing homologues **5** and **6** display better assignable ^{1}H-NMR spectra between +30 and −80°C. Below −20°C, two discrete *N*-methyl, and two C_5H_5, proton resonances appear in the spectrum of **5**, the coalescence temperature of the former lying at about +10°C, and for the latter between −10 and 0°C. The corresponding coalescence temperatures of the diamagnetic complex **6** (Ln = Lu) lie around −25 and at −56°C, respectively. The complete spectra of both complexes at +20 and −70°C are presented in Fig. 8a and Fig. 8b. Obviously, in both cases type **B** is realized at lower temperatures. As the ionic radii of the ions Yb^{3+} and Lu^{3+} do not differ significantly [13], a very similar coordination chemistry is actually expected for them. The significantly different coalescence temperatures of **5** and **6** are therefore most probably due to the different magnetic properties of the two complexes, and not to any significantly different activation parameters. To confirm this hypothesis experimentally, a detailed variable-temperature ^{1}H-NMR study involving precise (absolute) temperature measurements in steps of ca. 5°C, and the concomitant evaluation of $\Delta H^{\#}$ and $\Delta S^{\#}$, is currently underway.

One of the aims of the present contribution has been to demonstrate that appropriate use can be made of the paramagnetism of selected lanthanoid(III) ions such as Pr^{3+} or Yb^{3+} to confirm that, owing to the well-known, general lability of most Ln-to-ligand bonds, the molecular structure of Ln-complexes in solution may not necessarily agree with the structure deduced from a crystallographic X-ray study. In solution, rapid equilibria between different species lead frequently to the coalescence of relevant signals above, or even below the melting points of most available NMR-solvents. The intrinsic paramagnetism of a central lanthanoid ion often causes even wider separations of relevant signals than a paramagnetic NMR shift reagent. Thus, at

Table 7
^{13}C-NMR shifts (in ppm) of the compounds **4**, **6**, **7** and **11**

Sample	C_5H_5	$N(CH_3)_2$	α-CH_2	β-CH	γ-CH_2	δ-CH_3
4	106.3, 105.1	44.6	76.8	67.2	37.6	11.4
6	109.0	42.6	68.3	67.6	14.8	13.0
7	–	39.8	66.2	60.2	16.9	11.2
11	108.0	40.1	61.4	60.0	–	–
		35.2[a]			140.4[b]	129.0[c]

[a] NCH_2. [b] C_6H_5 (singlet). [c] C_6H_5 (multiplet).

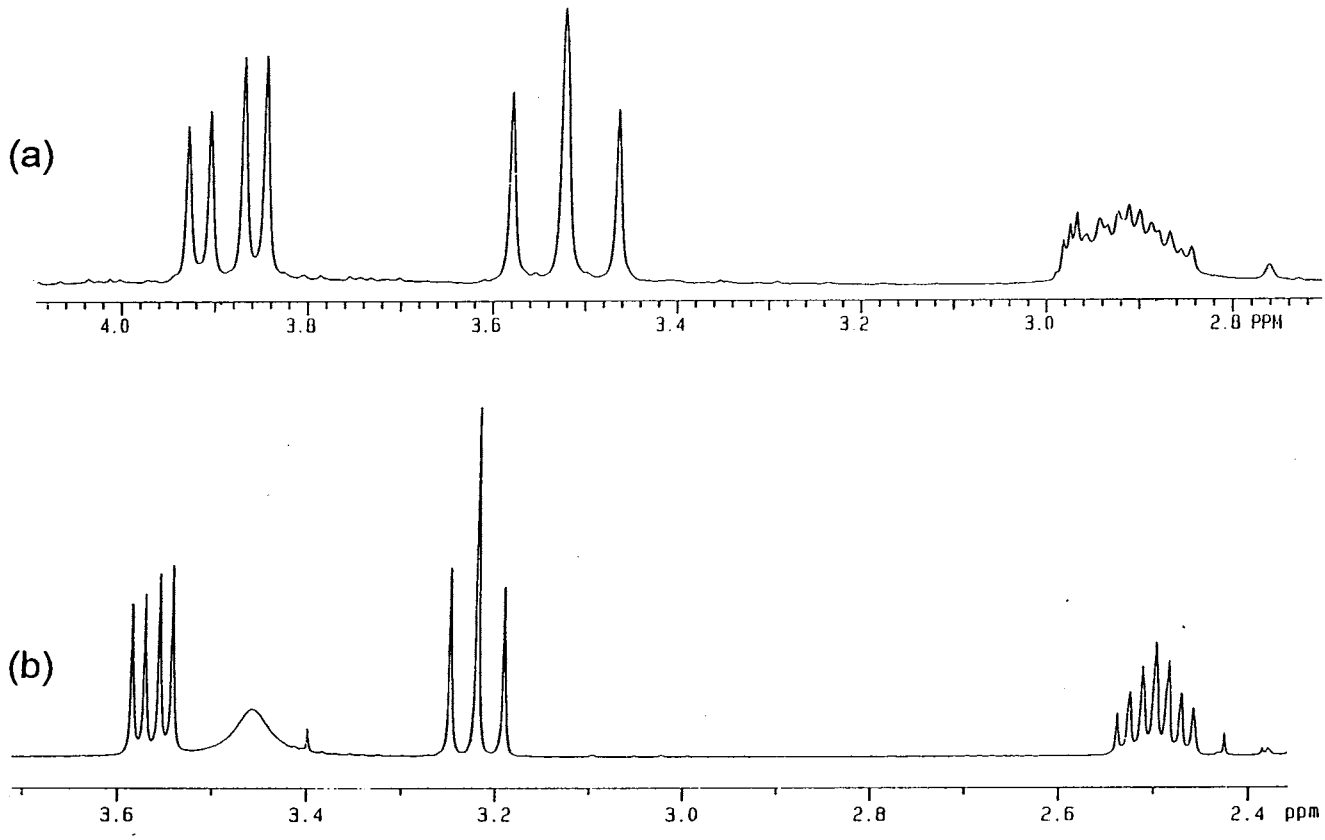

Fig. 5. Resonance patterns of the α-CH_2 and β-CH fragments of **6** (a) and the pure alcohol **7** (b).

-70°C the separation $\Delta\delta$ of the two C_5H_5 signals of **5** amounts to ca. 24 ppm, but to only 0.07 ppm for **6**. Similarly, $\Delta\delta(CH_3)$ of **5** is 19.4 ppm, but only 0.22 ppm for **6**. Consequently, the coalescence temperatures of paramagnetic **5** lie ca. 50 and 35°, respectively, higher than those of **6**. This result clearly suggests that the coalescence phenomena of numerous paramagnetic complexes could still be observable, while those of their diamagnetic homologues would be expected to occur below the melting point of the best NMR-solvents available.

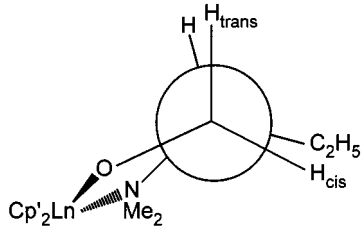

Fig. 6. Newman projection of the C^{α}–C^{β} bond of a chelating DMAB ligand (form **B**), following the X-ray structure of the Yb-complex with an -OCH_3 instead of the -$N(CH_3)_2$ group ([10]a).

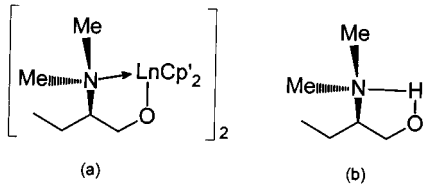

Fig. 7. Comparison of the five-membered rings present in type **B** complex of DMAB (a) and in the alcohol H-DMAB (b).

Finally, it should be recalled that the $CH_3C_5H_4$ ligands of **2**, **3**, **8** and **9** have tacitly been assumed to rotate as rapidly about their ring normals as the less bulky C_5H_5 ligands. While for the latter the appearance of only one ring proton resonance leaves no doubt in rapid rotation, the resonance pattern of a distinctly fixed $CH_3C_5H_4$ ligand would display just as many signals as a rapidly rotating ligand with two diastereotropic pairs of protons (vide supra). For the time being, we are not aware of any bis(cyclopentadienyl)lanthanoid complex whose (untied) ring ligands would have to be considered as spatially fixed. Even the cyclic ligands of the sterically strongly congested complex $[(Et_3SiC_5H_4)_3Pr\cdot NCMe]$ have been found [14] to rotate rapidly, while the four C_5H_4 proton resonances of the dinuclear complex $[O(Me_2SiC_5H_4)_2YbCl]_2$ [15] wherein the rings cannot rotate because of the presence of a Me_2Si tether are separated more widely from each other than in the spectrum of complex **9**. The quite impressive magnification of the diastereotropic splitting by the paramagnetism of the lanthanoid ion still deserves a theoretically based explanation.

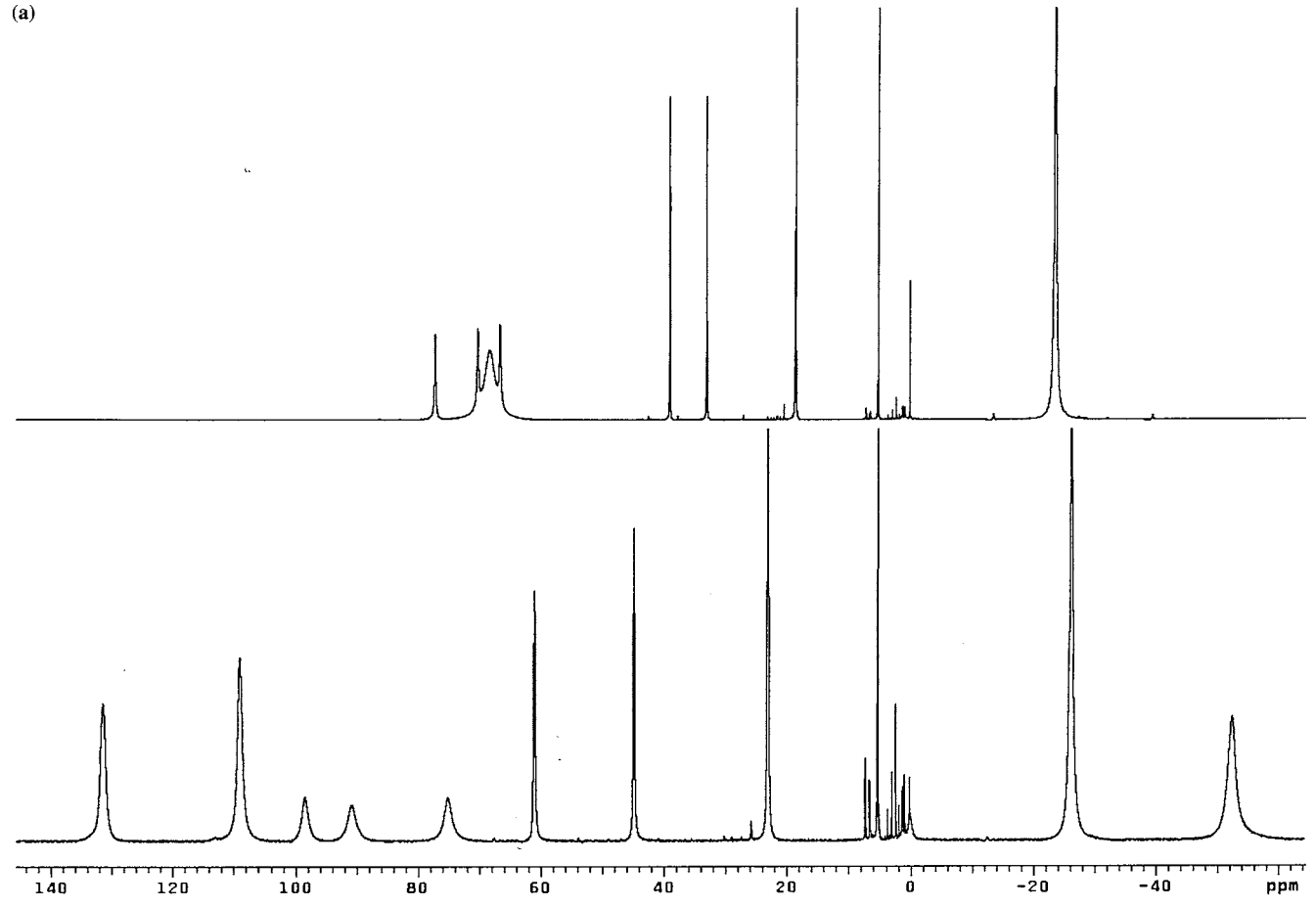

Fig. 8a. ^{1}H-NMR spectra of **5** at r.t. (top) and −70°C (bottom). See also Tables 4 and 5.

2.5. Experimental section

All operations were carried out under a strict N_2 atmosphere, using throughout oxygen-free, anhydrous solvents [10]. IR spectra were obtained on a Perkin Elmer IR 1720 instrument, and mass spectra on a Varian 311A spectrometer equipped with a Finnigan Spectro System MAT 188 data processing unit. NMR r.t. spectra (^{1}H and ^{13}C) were run either on a Varian Gemini 200 (200 MHz) or on a Bruker AM 360 spectrometer (360 MHz). Variable-temperature (VT) spectra (^{1}H) were obtained on a Varian Unity 400 instrument (400 MHz).

THF-free tris(cyclopentadienyl)lanthanoid complexes, [LnCp′$_3$], were prepared according to the literature [16]. Most of these complexes were purified by sublimation (e.g. at 180–210°C for [Yb(C_5H_5)$_3$], and at 200–230°C for [Pr(C_5H_5)$_3$]) in yields between 70 and 90%.

The ligand precursors (S)-(-)-2-methylbutanol, H-MB, and 2-(*N*-dimethylamino)ethanol, H-DMAE, were purchased from Fluka. (R)-(-)-2-(*N*-dimethylamino)butanol, H-DMAB, was prepared from (R)-(-)-2-amino-1-butanol (Merck), formic acid and formaldehyde following the method of Kaluszner and Galun [17] in a yield of 80% (b.p. 64°C) [10]. (R)-(+)-2-(*N*-methylbenzylamino)-1-phenylethanol, H-BMPE, was prepared following [18] from *N*-methylbenzylamine, *n*-butyl-lithium and (R)-(+)-styryloxide (yield: 96%).

2.5.1. Synthesis of **1** (also representative for the preparation of **3**–**6**)

544.2 mg (1.62 mmol) of Pr(C_5H_5)$_3$ was suspended in 50 ml of toluene at a temperature of −88°C. After adding dropwise a solution of 187.7 mg (1.6 mmol) of H-DMAB in 25 ml of toluene, the resulting solution is allowed to warmed up to r.t. and reduced to a volume of ca. 30 ml. After brief warming up to 40°C, filtration (P4 frit) and complete solvent evaporation, the resulting green residue is washed with 5 ml of cold *n*-hexane and dried in vacuo (8 h). Yield: 500 mg (81%) of a pale green solid. Elemental analysis $C_{16}H_{24}NOPr$ calcd. C 49.62, H 6.25, N 3.62; found: C 49.09, H 6.38, N 3.85%. **3** (yield: 91%), elemental analysis $C_{18}H_{28}NONd$ calcd. C 51.64, H 6.74, N 3.35; found: C 50.07, H 6.78, N 3.65%. **4** (yield: 85%), elemental analysis $C_{16}H_{24}NOSm$ calcd. C 48.44, H 6.10, N 3.53; found: C 48.03, H 6.10,

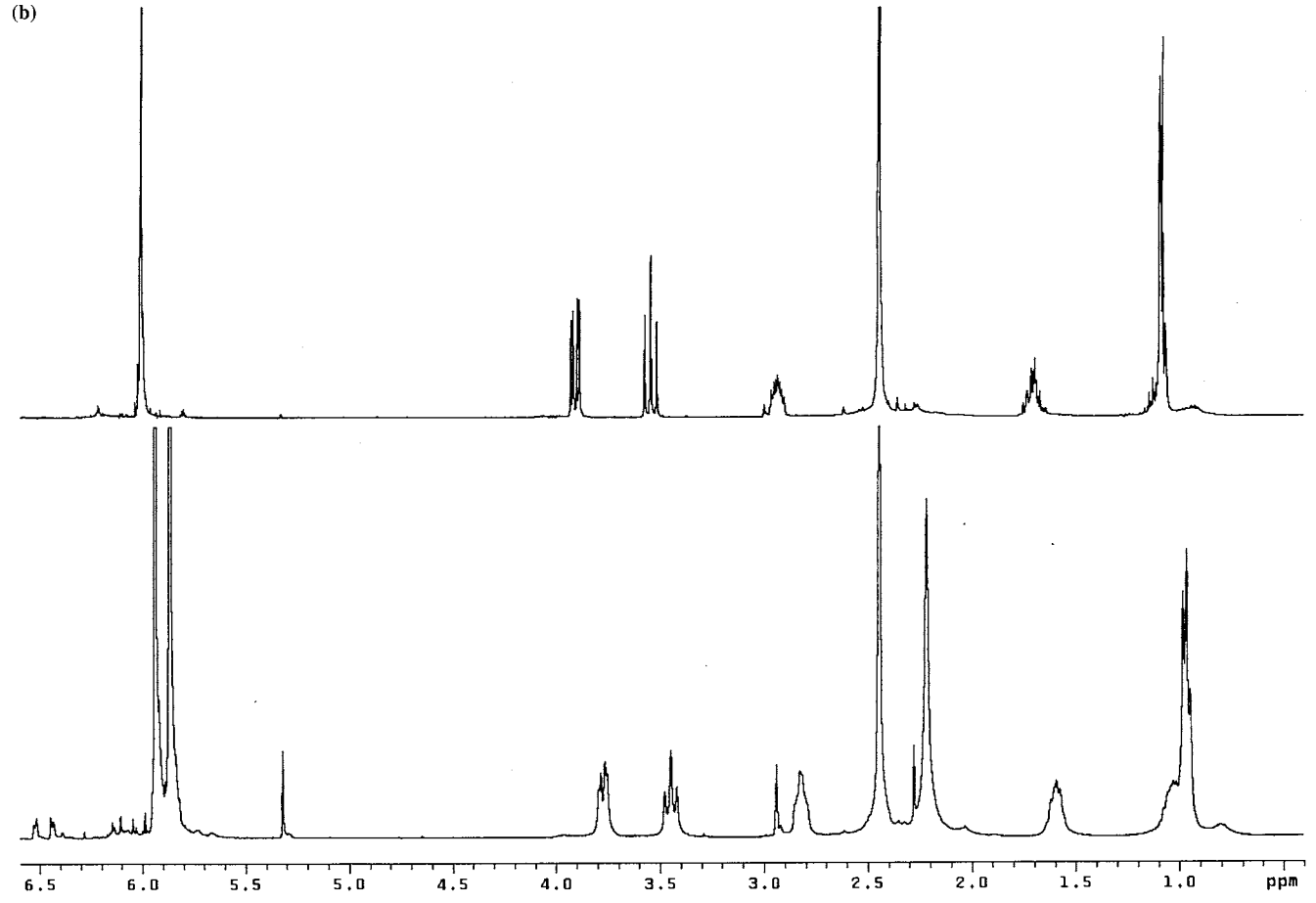

Fig. 8b. ^{1}H-NMR spectra of **6** at r.t. (top) and −70°C (bottom). See also Tables 4 and 5.

N 3.81%. **5** (yield: 83%), elemental analysis calcd. C 45.82, H 5.77, N 3.34; found: C 45.15, H 5.73, N 3.53%. **6** (yield: 85%), elemental analysis calcd. C 49.43, H 6.22, N 3.60; found C 46.54, H 6.09, N 4.24%.

2.5.2. Synthesis of *2*

464.5 mg (1.23 mmol) of $[Pr(CH_3C_5H_4)_3]$, 109.6 mg (1.23 mmol) of H-DMAE and 80 ml of toluene (in total); yield: 418.3 mg of **2** (90%). Elemental analysis $C_{14}H_{20}NOPr$ calcd. C 49.43, H 6.22, N 3.60; found C 48.54, H 6.04, N 4.14%. Synthesis of **3**: 470.1 mg (1.23 mmol) of $[Nd(CH_3C_5H_4)_3]$, 1.68 ml (144.1 mg = 1.23 mmol) of H-DMAB, 95 ml of toluene; yield: 468.6 mg (91%) of a light blue solid. Elemental analysis $C_{18}H_{28}NONd$ calcd. C 51.64, H 6.74, N 3.35; found C 50.07, H 6.78, N 3.65%.

2.5.3. Synthesis of *8* and *9* (example: *8*)

At −80°C, a solution of 153.5 mg (1.74 ml = 1.55 mmol) of H-MB in 30 ml of toluene is dropped slowly to a solution of 584.6 mg (1.55 mmol) of $(CH_3H_5H_4)_3Pr$ in 50 ml of toluene. Within 15 min, the colour changes from pale green to yellowish green. After continued stirring at room temperature (0.5 h), vacuum evaporation of one third of the solvent, filtration (P4 frit) and complete solvent removal, the solid residue is washed two times with 5 ml of *n*-hexane. After drying, 538.9 mg (yield: 90%) of a green powder is obtained. Elemental analysis $C_{17}H_{25}OPr$ calcd. C 52.86, H 6.52; found: C 51.74, H 6.41%. **9** (yield: 93%), elemental analysis $C_{17}H_{25}OYb$ calcd. C 48.80, H 6.02; found: C 45.09, H 5.70%.

2.5.4. Synthesis of *10-12* (example: *11*)

At −80°C, a solution of 478.5 g (2.0 mmol) of H-BMPE in 25 ml of toluene is added dropwise to a suspension/solution of 695.4 mg (2.0 mmol) of $[Sm(C_5H_5)_3]$ in 50 ml toluene. After continued stirring at room temperature, reduction of the volume to ca. 30 ml and warming up to ca. 40°C, filtration and solvent evaporation to a residual volume of 15 ml, 760.5 mg (yield: 73%) of pure **11** crystallized within 4 days at 4°C as yellow needles. Elemental analysis $C_{26}H_{28}NOSm$ calcd. C 59.96, H 5.42, N 2.69; found: C 56.73, H 5.53, N 2.55%. **10** (yield: 87%), elemental analysis $C_{26}H_{28}NOPr$ calcd. C 61.06, H 5.52, N 2.74; found: C 60.54, H 5.63, N 2.93%. **12** (yield: 75%). elemental analysis $C_{26}H_{28}NOYB$ calcd. C 57.46, H 5.19, N 2.58; found: C 59.31, H 5.60, N 3.01%.

*2.5.5. X-ray crystallography of **11***

Data were collected at 153 K on a Hilger and Watts Y290 diffractometer (Mo–K_α radiation and graphite monochromator). Heavy atoms were located by a three-dimensional Patterson synthesis, and subsequent difference Fourier and least-squares calculations have led to the positions of the C-, N- and O-atoms. The phenyl and cyclopentadienyl rings were refined as rigid bodies with fixed C–C distances of 139 and 142 pm, respectively. The $2\frac{1}{2}$ solvent (toluene) molecules present per dinuclear complex unit were also refined as rigid bodies with constant intra-ring C–C distances of 142 and of 154 pm for the exocyclic C–C σ-bond. For the C–C σ-bonds C50–C56, C60–C66 and C70–C76, the corresponding C(methyl)–C(ring, *ortho*) distances had to be fixed to 252 pm. For the refinement of the H-atoms, the C–H distances were fixed to 96 pm. All non-H atoms except C50 to C76 (of solvent molecules) were refined anisotropically [19].

Acknowledgements

Financial support by the BMBF, Bonn (Project Nr. 03DOO23B/8) and the M.U.R.S.T., Rome is gratefully acknowledged. We also thank S. Samba, K. Rechter and S. Formenti for their technical assistance.

References

[1] R. Kumar, M.L. Sierra, J.P. Oliver, Organometallics 13 (1994) 4285.
[2] (a) G. Massarweh, R.D. Fischer, J. Organomet. Chem. 444 (1993) 67. (b) J. Stehr, R.D. Fischer, J. Organomet. Chem. 459 (1993) 79. (c) W.-W. Ma, Z.-Z. Wu, R.-F. Cai, Z.-E. Huang, J. Sun, Polyhedron 16 (1997) 3723.
[3] For two earlier CD (circular dichroism) studies of organolanthanoid complexes see Refs. 2(b) and 9.
[4] See: (a) G.N. LaMar, W. DeW. Horrocks, Jr., R.H. Holm (Eds.) NMR of Paramagnetic Molecules, Academic Press, New York, 1971. (b) R.D. Fischer, in: T.J. Marks, R.D. Fischer (Eds.), Organometallics of the f-Elements, D. Reidel, Dordrecht, 1979, p. 337, and further references cited therein. (c) I. Bertini, C. Luchinat, NMR of Paramagnetic Molecules in Biological Systems, Benjamin-Cummings, Menlo Park, 1986.
[5] W.J. Evans, R. Anwander, U.H. Berlekamp, J.W. Ziller, Inorg. Chem. 34 (1995) 3586.
[6] G.B. Deacon, B.M. Gatehouse, S.N. Platts, D.L. Wilkinson, Aust. J. Chem. 40 (1987) 907.
[7] Use of racemic H-DMAB for the synthesis should in principle lead to a mixture of two NMR spectroscopically nonequivalent isomers.
[8] While the $\{Me_2NCH_2\}$ fragment will undergo rapid (on the NMR time scale) inversion, the $\{Cp'_2Ln(O)_2\}$ fragment is influenced here by two equivalent chirogenic centres.
[9] For the more recent NMR study of a related, likewise chiral $Cp_2Sm(III)$-derivative, see: A. Steudel, J. Stehr, E. Siebel, R.D. Fischer, J. Organomet. Chem. 510 (1996) 197.
[10] A. Steudel, Doctoral Dissertation, Universität Hamburg (Germany) 1997 (a) p. 19. (b) ibid. p. 32. (c) ibid. p. 83.
[11] See: M. Hesse, H. Meier, B. Zeeh, Spektroskopische Methoden in der Organischen Chemie, Thieme, Stuttgart, 1987, p. 101.
[12] H. Schumann, F. Erbstein, R. Weimann, J. Demtschuk, J. Organomet. Chem. 536–537 (1997) 541.
[13] See: R.D. Shannon, Acta Crystallogr. A32 (1976) 751.
[14] M. Sievers, R.D. Fischer, unpublished results.
[15] J. Gräper, R.D. Fischer, G. Paolucci, J. Organomet. Chem. 471 (1994) 87.
[16] W.A. Herrmann, F.T. Edelmann (Eds.), Synthetic Methods of Organometallic and Inorganic Chemistry, vol. 6, Thieme, Stuttgart, 1997, p. 68.
[17] A. Kaluszner, A.B. Galun, J. Org. Chem. 26 (1961) 3536.
[18] C.E. Harris, G.B. Fisher, D. Beardsley, L. Lee, C.T. Goralski, L.W. Nicholson, B. Singaram, J. Org. Chem. 59 (1994) 7746.
[19] Full details of the crystal structure determination of **11** have been deposited at the Fachinformationszentrum Karlsruhe GmbH, D-76344 Eggenstein-Leopoldshafen, Germany, and can be obtained on quoting the depository number CSD-406283.